Published in final edited form as:
Mol Cell. 2008 November 7; 32(3): 426–438. doi:10.1016/j.molcel.2008.10.012.

Hierarchical Regulation of WASP/WAVE Proteins

Shae B. Padrick[1,*], **Hui-Chun Cheng**[1,*], **Ayman M. Ismail**[1,*], **Sanjay C. Panchal**[1], **Lynda K. Doolittle**[1], **Soyeon Kim**[1], **Brian M. Skehan**[2], **Junko Umetani**[1], **Chad A. Brautigam**[1], **John M. Leong**[2], and **Michael K. Rosen**[1]

1*Howard Hughes Medical Institute and Department of Biochemistry, University of Texas Southwestern Medical Center, Dallas, Texas 75390.*

2*Department of Molecular Genetics and Microbiology, University of Massachusetts Medical School, Worcester, MA 01655.*

SUMMARY

Members of the Wiskott-Aldrich Syndrome Protein (WASP) family control actin dynamics in eukaryotic cells through stimulating the actin nucleating activity of the Arp2/3 complex. The prevailing paradigm for WASP regulation invokes allosteric relief of autoinhibition by diverse upstream activators. Here we demonstrate an additional level of regulation that is superimposed upon allostery: dimerization increases the affinity of active WASP species for Arp2/3 complex by up to 180-fold, greatly enhancing actin assembly by this system. This finding explains a large and apparently disparate set of observations under a common mechanistic framework. These include WASP activation by the bacterial effector EspFu and a large number of SH3 domain proteins, the effects on WASP of membrane localization/clustering and assembly into large complexes, and cooperativity between different family members. Allostery and dimerization act in hierarchical fashion, enabling WASP/WAVE proteins to integrate different classes of inputs to produce a wide range of cellular actin responses.

INTRODUCTION

Dynamic rearrangements of the actin cytoskeleton are an integral part of many cellular processes including migration, adhesion, establishment and maintenance of polarity, and vesicle trafficking (Chhabra and Higgs, 2007; Pollard and Borisy, 2003; Takenawa and Suetsugu, 2007). Defects in cytoskeletal structure and dynamics contribute to a variety of diseases, including cancer, developmental disorders, immunodeficiencies and bacterial/viral infection (Munter et al., 2006; Ochs and Thrasher, 2006; Yamazaki et al., 2005). Actin dynamics are regulated both spatially and temporally by a wide array of extracellular signals. Members of the Wiskott-Aldrich Syndrome Protein (WASP) family play central roles in processing these signals to control actin architecture and rearrangements (Chhabra and Higgs, 2007; Pollard and Borisy, 2003; Stradal and Scita, 2006; Takenawa and Suetsugu, 2007). WASP proteins exert their function by controlling the ubiquitous actin nucleation factor, Arp2/3 complex. The family includes WASP, the widely expressed neuronal-WASP (N-WASP), and several Scar/WAVE proteins (Campellone et al., 2008; Linardopoulou et al.,

Corresponding Author: Dr. Michael K. Rosen, Tel: (214)-645-6361, Fax: (214)-645-6291, E-mail: Michael.Rosen@UTSouthwestern.edu.
*These authors contributed equally to this work

2007; Takenawa and Suetsugu, 2007). WASP proteins are themselves regulated by numerous diverse signals, including Rho family GTPases, phospholipids, kinases, many SH3 domain-containing proteins and both bacterial and viral pathogen proteins (Pollard and Borisy, 2003; Takenawa and Suetsugu, 2007). Integration of these signals results in the precise spatial and temporal control over actin dynamics that is necessary for cell organization and function.

The prevailing model for WASP regulation invokes inhibitory intramolecular contacts between the regulatory GTPase binding domain (GBD) and the activity-bearing VCA domain of the protein (Goley and Welch, 2006; Leung and Rosen, 2005; Papayannopoulos et al., 2005; Pollard, 2007; Stradal and Scita, 2006; Takenawa and Suetsugu, 2007). These autoinhibitory interactions block VCA stimulation of Arp2/3 complex. WASP activators relieve autoinhibition allosterically by disrupting the GBD-VCA contacts, enabling the VCA to activate Arp2/3 complex. An analogous mechanism involving intermolecular inhibition of the VCA has also been proposed for regulation of WAVE proteins (Eden et al., 2002).

The allosteric model originally derived from studies of N-WASP activation by Cdc42, a Rho family GTPase (Kim et al., 2000; Miki et al., 1998; Rohatgi et al., 1999). Structural and biophysical studies have shown that it can explain the regulation of WASP and N-WASP by many ligands, including Cdc42, PIP_2 (but see below), kinases/phosphatases, SH2 domain containing proteins, and bacterial pathogen proteins (Kim et al., 2000; Prehoda et al., 2000) (Cheng et al., 2008; Leung and Rosen, 2005; Peterson et al., 2004; Torres and Rosen, 2003).

However, many reported observations on WASP proteins are not readily explained by allostery alone. First, although a single repeated element in the pathogen protein EspFu/TccP can modestly activate WASP by displacing the GBD from the VCA, multi-repeat fragments result in much stronger stimulation of Arp2/3 complex (see below, and (Garmendia et al., 2006; Sallee et al., 2008)). Second, the ability of WASP proteins to stimulate Arp2/3 complex can be increased by numerous SH3-containing ligands, which bind the large (~125 residues), structurally disordered proline-rich domain that connects the GBD to the VCA (Takenawa and Suetsugu, 2007). It is difficult (albeit not impossible) to envision how SH3 binding to this long, flexible loop could destabilize the GBD-VCA domain to which it is attached. Third, while the isolated WASP VCA can activate Arp2/3 complex, the fusion of the VCA to dimeric glutathione S-transferase (GST) is a much stronger activator (Higgs and Pollard, 2000). Fourth, direct and indirect clustering of WASP proteins at membranes *in vitro* and *in vivo* can increase Arp2/3-mediated actin assembly, independent of obvious allosteric rearrangements (Castellano et al., 1999; Papayannopoulos et al., 2005; Rivera et al., 2004; Yarar et al., 2007). Finally, WASP and N-WASP are often reported to function within large assemblies that are organized around multi-valent adaptor proteins (Ho et al., 2004; Tehrani et al., 2007; Yarar et al., 2007). *In vitro*, incorporation of N-WASP into these assemblies can increase activity toward Arp2/3 complex independent of obvious allosteric drivers (Tehrani et al., 2007) or sensitize the system toward allosteric activation (Ho et al., 2004). These various observations suggest that important mechanism(s) of regulating the activity of WASP proteins toward Arp2/3 complex, in addition to allostery, remain to be discovered.

Here we show that dimerization of active WASP species provides an additional layer of regulation beyond allostery. VCA dimers bind Arp2/3 complex in 1:1 fashion (2 VCAs per Arp2/3) with 100–180-fold higher affinity than VCA monomers. This finding leads to a hierarchical model for WASP/WAVE regulation in which an inner layer of allostery controls VCA access and an outer layer of dimerization (or more generally oligomerization) significantly enhances potency toward Arp2/3 complex. This model provides a common mechanistic framework that explains the wide range of apparently disparate data on WASP regulation listed above. Probabilistic arguments illustrate how oligomerization can enhance

the dimerization effect to control WASP activity and potentiate the effects of allosteric inputs, explaining the prevalence of large assemblies throughout WASP biology.

RESULTS

Dimerization Increases VCA Affinity for Arp2/3 Complex by Over 100-Fold

Higgs and Pollard reported that in pyrene-actin assembly assays a GST-fusion of the WASP VCA has a much greater activity toward Arp2/3 complex than the isolated VCA (Higgs and Pollard, 2000). GST forms very high affinity dimers in solution (K_D < 1 nM, not shown), and these authors suggested that dimeric VCA might have higher activity than monomer. As shown in Figure 1A, this effect is also observed for the N-WASP and WAVE1 VCAs, whose GST-fusions have much greater activity than monomers. This effect is due to dimerization rather than attachment to GST, since purified GST:GST-VCA heterodimers have much lower activity than homodimer (Fig. S1). Further, chemically crosslinked WASP VCA (xlWASP VCA) and the rapamycin-mediated heterodimer of FKBP-VCA and mTOR-VCA (Banaszynski et al., 2005) show activity comparable to GST-VCA (Fig. 1B). Most assays of Arp2/3 activation reported in the literature have been performed in 50 mM KCl buffer. Under these conditions, 10–100 nM concentrations of WASP family VCAs produce significant activation of Arp2/3 complex. However, at physiologic salt (150 mM KCl), the activity of N-WASP VCA is substantially reduced and WASP and WAVE1 VCAs are virtually inactive, while GST-VCAs retain substantial activity (Fig. 1B, C and not shown). Thus, dimerization of the VCA element appears to be a general mechanism of increasing activity of WASP family proteins toward Arp2/3 complex that is likely important under physiologic conditions.

We next asked how dimerization increases VCA activity. One possibility was that filament barbed end binding by one V region (Co et al., 2007) increased the local F-actin concentration relative to the second VCA and its bound Arp2/3 complex. However, a GST-VCA mutant impaired in barbed end binding has activity comparable to wild type (Fig. S2), arguing against this model. Instead we asked whether the nature of the Arp2/3-VCA interaction is changed when VCA is dimeric. Current models of active Arp2/3 invoke only a single VCA binding site in the complex (Chhabra and Higgs, 2007; Goley and Welch, 2006; Pollard, 2007; Stradal and Scita, 2006). We determined the stoichiometry of the complex between GST-WASP VCA dimers and Arp2/3 using two different methods. In sedimentation velocity analytical ultracentrifugation experiments (Fig. 2A, Fig. S3), GST-WASP VCA and Arp2/3 had their expected masses of 73.7 kDa (calculated dimer mass = 70.2 kDa) and 208 kDa (calculated mass = 224 kDa) when analyzed separately. For mixtures with GST-VCA:Arp2/3 ratios greater than 2:1 (in monomer units), we observed two species, consistent with the GST-WASP VCA dimer (experimental mass = 73.9 kDa) and a 2:1 complex of GST-WASP VCA and Arp2/3 (experimental mass = 286 kDa, calculated mass = 294 kDa). The experimentally derived masses correspond well to the calculated masses, and the data clearly do not support the presence of a 2:2 complex of GST-WASP VCA and Arp2/3 (calculated mass = 518 kDa). Analyzing the data, explicitly accounting for complex association also yielded a high affinity 2:1 complex (see Supplemental Materials). When experiments were performed at a GST-VCA:Arp2/3 ratio of 1.4:1, the smaller species was not observed and the sedimentation coefficient of the larger species decreased, suggesting a mixture of free Arp2/3 and the 2:1 complex. We also measured the mass of the complex using multi-angle static light scattering, which yielded a value of 302 kDa (Fig. 2B), again indicating 2:1 stoichiometry. Thus, by two independent analytical methods we find that a VCA dimer binds a single Arp2/3 complex.

We used a fluorescence competition binding assay to measure the affinities of VCA monomers and GST-VCA dimers for Arp2/3 complex (Fig. 2C, Fig. S4) (Marchand et al., 2001). The affinities for monomer VCAs are similar to those reported previously, ranging from 1.6 μM to 4.4 μM (Marchand et al., 2001;Zalevsky et al., 2001). The dimers all had substantially higher

affinity, between 9 nM and 29 nM, when data were fit to a model with 2:1 stoichiometry of GST-VCA to Arp2/3 complex (Fig. 2C, Fig. S4). This corresponds to an increase in affinity of 100-, 150- and 180-fold for WASP, WAVE1 and N-WASP, respectively.

Increased affinity is also manifest *in vivo*. Small amounts of Arp2/3 can be precipitated with Ni^{2+}-affinity resin from HEK293 cells co-expressing His6-tagged FKBP-VCA and Flag-tagged mTOR-VCA, but dimerization of the VCAs with rapamycin increases the precipitated Arp2/3 by more than three-fold (Fig. 2D). This effect requires two VCAs in the rapamycin-mediated complex, as His-tagged FKBP precipitates mTOR-VCA but very little Arp2/3 under similar conditions.

To test whether increased affinity is sufficient to account for the increased actin assembly activity of the dimers, we measured the activities of N-WASP VCA and GST-N-WASP VCA at a range of concentrations (Fig. S5). At saturation, the kinetics of actin assembly and concentration of filament barbed ends produced by monomer and dimer are essentially identical, similar to observations with the WASP VCA (Higgs and Pollard, 2000). This suggests that differences at lower concentrations are principally due to the differences in VCA affinity for Arp2/3 complex (which will not have an effect at saturation). As described in the Supplementary Materials (see also Fig. S6), kinetic simulations of actin assembly using a previously reported model (Zalevsky et al., 2001) lead to the same conclusion. These combined data show that dimerization represents a general mechanism of increasing the activity of WASP family VCAs by greatly enhancing their affinity for Arp2/3 in a 2:1 complex.

How does dimerization increase affinity of the VCA for Arp2/3 complex? Dimerization does not induce structural changes in the VCA (Fig. S7) that could account for higher activity. An alternative mechanism stems from behavior of the cortactin protein, which can bind Arp2/3 complex simultaneously with VCA peptides, utilizing an element analogous to the A region of the VCA (termed NtA) (Fig. S8 and (Weaver et al., 2002)). Thus, Arp2/3 complex appears to have two binding sites for A region peptides, one favored by VCA and one favored by cortactin, that can be engaged simultaneously. In the context of a VCA dimer, the cortactin site could be engaged by the second VCA, increasing affinity. To test this possibility, we examined the interactions of rhodamine-NtA (rNtA) with Arp2/3 complex in the presence of competitors (Fig. 2E). Unlabeled NtA potently displaces rNtA from Arp2/3 complex (K_D = 17 nM), but monomeric VCA is much less effective (Fig. 2E). Thus, the cortactin site on Arp2/3 complex binds NtA tightly but VCA only modestly. In contrast, dimeric xlWASP VCA displaces rNtA very effectively (K_D = 70 nM, similar to that derived from displacement of fluorescent VCA; Fig. 2C). The simplest explanation for these data is that xlWASP VCA simultaneously engages both the canonical VCA and cortactin binding sites on Arp2/3 complex (Fig. 2F). Thus, dimerization of WASP increases affinity for Arp2/3 complex by enabling multivalent binding.

If the effect of dimerization applies to full-length WASP proteins, then ligands capable of assembling multiple active WASPs on a single scaffold should act as potent enhancers of activity. We note that thermodynamics dictates that since dimerization increases the affinity of WASPs for Arp2/3 complex, Arp2/3 complex must identically increase the affinity of WASPs for dimerizer molecules. Thus, such dimerizer-WASP-Arp2/3 assemblies should form in a highly cooperative fashion. To better understand the behavior of such systems we modeled the activation of Arp2/3 complex by WASP in the presence of a bivalent ligand. This modeling predicted several characteristic features in a titration of a dimerizing ligand into WASP (Fig. 3, Fig. S9). First, for low WASP concentrations a dimerizer can produce activity substantially above that of the corresponding VCA, due to the higher affinity of the $(WASP)_2$ species for Arp2/3 complex (Fig. 3A). We refer to this phenomenon as “hyperactivation” throughout the text. Second, titration of a dimerizer into WASP will give a bell-shaped activity profile, distinct

from the monotonic increase in activity induced by a monomeric activator (Fig. 3A). At low dimerizer concentration, little WASP is bound and activity is low (Fig. 3D-1). For intermediate concentrations, some dimerizer molecules engage two WASP molecules, and this high affinity $(WASP)_2$ species will have activity beyond that of the VCA (Fig. 3D-2). At high dimerizer concentration, most WASP is bound, but the probability of two WASP molecules engaging the same dimerizer molecule is low (Fig. 3D-3). Therefore, activity will be comparable to that of the monovalent activator or of the free VCA. Together, these effects produce a bell-shaped activity profile. Analogous behavior is also observed in titrations involving a constitutively active WASP mutant (Fig. S9A). Finally, a mono-valent version of the dimerizer will compete for WASP binding, actively blocking dimerizer-induced hyperactivation (Fig. 3B, 3D-4, Fig. S9B). With these predictions in hand, we asked if dimerization might account for some of the unexplained WASP/N-WASP activation phenomena described in the Introduction.

Dimerization generates inter-repeat cooperativity in WASP/N-WASP activation by EspFu

Enterohaemorrhagic *E. coli* (EHEC) is an important food-borne human pathogen that subverts the actin cytoskeleton of host cells during infection (Campellone et al., 2004; Garmendia et al., 2006; Garmendia et al., 2004). EHEC induces filamentous actin “pedestals” at sites of bacterial attachment by injecting the proteins Tir and EspFu into the eukaryotic cytoplasm. Tir inserts into the plasma membrane beneath the bound bacterium and recruits EspFu, which in turn binds and activates N-WASP. EspFu is composed of an N-terminal translocation sequence followed by 2 to 7.5 repeats of 47 residues (Campellone et al., 2004; Garmendia et al., 2004; Garmendia et al., 2005).

We recently showed that a single repeat of EspFu (1R) allosterically activates WASP/N-WASP by binding the GBD and releasing the VCA (Cheng et al., 2008). However, two repeats (2R) have significantly greater activity (Garmendia et al., 2006; Sallee et al., 2008), even when normalized for total repeat concentration (Fig. 5A). Thus, repeats cooperatively promote actin assembly. Cooperativity does not involve inter-repeat effects on the affinity of EspFu for N-WASP, since isothermal titration calorimetry (ITC) measurements show that 1R (the fourth repeat) and $2R_C$ (identical repeats four and five) bind with indistinguishable affinity but 2-fold different stoichiometry ($K_D = 35 \pm 5$ nM and 39 ± 2 nM, respectively, (Cheng et al., 2008) and data not shown) to an autoinhibited C-terminal fragment of N-WASP (N-$WASP_C$, Fig. S10). We asked whether cooperativity arises from assembly of two active WASP proteins on 2R, producing a dimer with high affinity for Arp2/3 complex. Titration of 1R into N-$WASP_C$ produces a monotonic increase in activity (defined in Methods) approaching that of free VCA, as expected for a ligand that relieves autoinhibition (Fig. 4A). In contrast, titration with 2R produces a bell-shaped activity profile with a peak well above that of free VCA (Fig. 4A). For 25 nM N-$WASP_C$, activity increases rapidly as 2R is added, peaks at 50 nM 2R, then decreases as 2R is increased further and plateaus near 1 μM. The decrease in activity at high concentration is not due to non-specific inhibition, as 500 nM 2R has no effect on VCA-mediated actin assembly (not shown). Moreover, the 1R and 2R titrations plateau at an activity near that of free VCA, suggesting that high concentrations of either fragment produce monomeric, allosterically activated N-$WASP_C$. Similar behavior is observed using $2R_C$, which has a three-fold tighter affinity for N-$WASP_C$, and also for a titration performed at physiologic salt concentration (Fig. S11).

Hyperactivation of N-$WASP_C$ by 2R can be blocked by addition of 1R, which competes with 2R for N-$WASP_C$ with comparable affinity (Fig. 4B). As in the 2R titration, the final activity in this 1R back titration is near that of free VCA. These data show that 1R is not merely a weaker activator than 2R (cf. Fig. 4A), but rather can actively block hyperactivation by 2R. Together, these data support a model where inter-repeat cooperativity in EspFu results from dimerization of active N-WASP, yielding a higher potency activator of Arp2/3 complex.

We next asked whether inter-repeat cooperativity is important in pedestal assembly in mammalian cells. We used an N-terminal fragment of Tir, fused to fragments of EspFu, to bypass membrane recruitment of EspFu by Tir and allow direct analysis of actin assembly activity in cells (previously described in (Cheng et al., 2008)). A single repeat of EspFu consists of a 33 residue N-WASP binding element (W) and a 14 residue proline-rich segment (P) (Cheng et al., 2008). We expressed Tir fusions containing no EspFu fragment (TirΔC), WP (=1R) or WPW. Treatment of cells expressing WPW with intimin-expressing *E. coli* produced numerous clusters of Tir and F-actin coincident with bound bacteria (Fig. 1D). In contrast, treatment of cells expressing WP generated clusters of Tir without associated F-actin, similar to TirΔC, indicating that the weaker activation of N-WASP by a single EspFu repeat observed *in vitro* is incapable of promoting detectable actin assembly in this cell-based assay. Thus, cooperativity between EspFu-bound N-WASP proteins appears to be important in assembling actin in cells.

A five repeat EspFu fragment (5R) has a somewhat higher activity than 2R (Fig. 5A), such that the relative activities are $1R \ll 2R_C < 5R$. Simple statistics can explain this effect (see Supplemental Materials). If one compares different *n*-repeat constructs at a fixed total repeat concentration and low occupancy of repeats by N-WASP (e.g. $[\text{N-WASP}] < K_{D,\ \text{N-WASP}}$), the relative concentration of $(WASP)_2$ complexes scales as (n-1). Therefore, more repeats will give higher activity, potentially explaining the fact that in most sequenced EHEC serotypes, EspFu has three or more repeats (Garmendia et al., 2005). An analogous argument suggests that higher-order oligomerization should generally enhance the activity of WASP proteins by increasing the probability that two active species will be proximal (see Discussion). Our combined data on EspFu indicate that EHEC has evolved two mechanistically distinct but coupled activities to drive actin assembly: allosteric release of the N-WASP VCA and oligomerization of active N-WASP to increase potency toward Arp2/3 complex.

Dimerization contributes to enhancement of WASP/N-WASP activity by SH3 domain proteins

Over 30 SH3 proteins have been reported to bind WASP, N-WASP and/or the WAVEs (see (Takenawa and Suetsugu, 2007) for a fairly complete list). These interactions occur through the 100–200 residue proline-rich region found in all family members. Many SH3-containing ligands have been demonstrated to enhance the activity of WASP and/or N-WASP toward Arp2/3 complex in actin assembly assays *in vitro*, including Nck (Rohatgi et al., 2001), Abi1 (Innocenti et al., 2005), Grb2, Fyn, PI 3-kinase p85, PLCγ, WISH (Fukuoka et al., 2001), FBP17 (Tsujita et al., 2006), SNX9 (Yarar et al., 2007) and PACSIN/syndapin (see below). In virtually all cases, enhancement was achieved with ligands containing multiple SH3 domains. This multiplicity resulted from self-association of the ligands, multiple SH3 domains in the monomeric ligand or the use of GST-SH3 fusions. Approximately 10% of WASP is active in solution, even in the absence of allosteric activators (Fukuoka et al., 2001; Leung and Rosen, 2005; Prehoda et al., 2000). Thus, oligomerization of WASP proteins through interactions with multivalent SH3-containing ligands might create dimers of active WASP.

To separate relief of autoinhibition from dimerization/oligomerization, we generated a mutant of N-WASP_C (N-WASP_C*, L232P in the GBD, Fig. S10), where autoinhibitory regulation is disrupted (Devriendt et al., 2001). N-WASP_C* has a nearly identical activity toward Arp2/3 complex as VCA alone (not shown), and is not further activated by excess Cdc42-GMPPNP (not shown). We then asked whether various SH3 proteins affect N-WASP_C* stimulation of Arp2/3 complex. The first was an SH3 containing fragment of Nck (Nck_F). While Nck_F has no effect on actin assembly through N-WASP_C*, the GST-Nck_F fusion increases activity substantially, hyperactivating the constitutively active mutant (Fig. 6A). GST-Nck_F has no effect on activity of the isolated VCA. Hyperactivation of N-WASP_C* requires Nck_F dimerization, since GST:GST-Nck_F heterodimers are largely inactive (Fig. S12). Importantly,

NckF monomer can partially block enhancement by the GST-Nck fusion, strongly suggesting that monomer can bind N-WASP$_C$*. Thus binding without oligomerization is insufficient to produce hyperactivation.

We next examined PACSIN2, an N-WASP ligand from the PCH family, many of whose members bind and/or activate WASP proteins (Takenawa and Suetsugu, 2007). PCH proteins contain an N-terminal F-BAR domain, which forms a constitutive homodimer, and a C-terminal SH3 domain (Shimada et al., 2007). As with GST-Nck$_F$, PACSIN2 hyperactivates N-WASP$_C$* (Fig. 4C). A GST-fusion of the PACSIN2 SH3 domain hyperactivates similarly, suggesting that this effect stems from the dimeric SH3 domain rather than particular properties of the PACSIN2 N-terminus (not shown). Analogous to the 2R fragment of EspFu, titration of PACSIN2 produces a bell-shaped activity profile (Fig. 4C). The degree of activation is not as high as with 2R, likely due to a lower affinity for N-WASP (see Discussion). Again, hyperactivation is blocked by excess SH3 monomer at concentrations that have no effect on N-WASP$_C$* alone (Fig. 4D).

These data show that even when autoinhibitory contacts are eliminated, dimeric SH3 domains can further increase the ability of N-WASP to stimulate Arp2/3 complex. This finding is consistent with a model in which dimeric/oligomeric WASP proteins assembled by SH3 dimers more potently activate the Arp2/3 complex than monomers. Thus, dimerization/oligomerization may be a significant component of SH3-mediated activation of WASP proteins.

The dimerization effect contributes to N-WASP activation by PIP$_2$

The lipid PIP$_2$ (phosphatidylinositol 4,5-bisphosphate), a known activator of WASP proteins (Higgs and Pollard, 2000; Prehoda et al., 2000; Rohatgi et al., 1999), binds to a basic peptide segment (B) N-terminal to the GBD (Prehoda et al., 2000). Prevailing mechanisms of N-WASP activation by PIP$_2$ focus on relief of inhibition (Papayannopoulos et al., 2005; Suetsugu et al., 2001). Indeed, PIP$_2$ can displace B-GBD from VCA (Rohatgi et al., 2000), demonstrating that relief of autoinhibition is a component of PIP$_2$-mediated activation of WASP proteins. Intriguingly, N-WASP proteins recruited to moving PIP$_2$-rich vesicles have a high local density, such that their spacing (< 5 nm (Co et al., 2007)) is less than the spacing predicted between the SH3 domains in the PACSIN2 dimer (~16 nm assuming a disordered F-BAR-SH3 linker) (Miller et al., 1967). This implies that high density WASP molecules on PIP$_2$ vesicles may act as dimers and more potently activate Arp2/3 complex. A similar argument has recently been made for the Arp2/3 activator from Listeria monocytogenes, ActA, which is expressed at high density on the bacterial surface (Footer et al., 2008). Thus, we asked whether the dimerization effect could contribute to PIP$_2$-mediated activation.

To separate relief of autoinhibition from the clustering of N-WASP on the surface of vesicles, we created a construct which fused the basic region to N-WASP$_C$ and deleted much of the GBD, creating a construct capable of binding PIP$_2$ but lacking allosteric regulation (N-WASP$_{BC}$*, Fig. S10). N-WASP$_{BC}$* has a somewhat lower activity than free VCA (Fig. 4E), possibly due to inhibitory interactions of the basic region with Arp2/3 (Suetsugu et al., 2001) or the acidic region. However, addition of high density PIP$_2$ vesicles (20% mole fraction), hyperactivates N-WASP$_{BC}$* (Fig. 4E). Activation is dose dependent, with 2μM PIP$_2$ producing substantially more activity than VCA alone. This concentration of PIP$_2$ does not affect activity of the free VCA (not shown).

If hyperactivation is the result of bringing multiple VCA domains into close proximity, then the effect should be sensitive to PIP$_2$ density on vesicles. To test this possibility we used vesicles with different PIP$_2$ densities to activate N-WASP$_{BC}$*. These vesicles were used at concentrations of 2 μM PIP$_2$ in solution, but at differing carrier lipid concentrations (see

scheme 1 in Fig. 4F). Here, hyperactivation decreases with decreasing PIP_2 density, such that 8% PIP_2 vesicles do not hyperactivate N-$WASP_{BC}$* (Fig. 4F). To test if the loss of hyperactivation is simply due to increased carrier lipid, we mixed preformed 20% PIP_2 vesicles and carrier vesicles. Since the vesicles do not fuse, the density of PIP_2 on individual vesicles does not change from the parent preparations, but total lipid concentrations can be matched to the density titration above (see scheme 2 in Fig. 4F). In this experiment, hyperactivation is largely maintained, suggesting that the effect requires high PIP_2 density.

A previous study showed that at higher salt conditions binding of N-WASP to vesicles was dependent on PIP_2 density (Papayannopoulos et al., 2005). To distinguish activation due to vesicle binding from activation due to close proximity of VCAs on the vesicle surface, we measured N-WASP binding to vesicles as a function of PIP_2 density under conditions of the actin assembly assays (see Supplemental Methods). We quantified the amount of N-$WASP_B$ (Fig. S10) that co-sedimented with sucrose loaded PIP_2 vesicles. As shown in Figure 4G and Figure S13, binding does not decrease at reduced PIP_2 density, and may even increase. Thus, PIP_2 vesicle binding and activation are not correlated in our system. Instead, the data are consistent with high potency activation of Arp2/3 by closely spaced VCAs on vesicles, an effect that is lost when VCAs are spread out over a greater area. This effect of clustering could contribute to the activation of WASP proteins by PIP_2 and membrane localization in general.

Cooperativity between N-WASP and WAVE1 through heterodimerization

WASP and WAVE proteins often have distinct localization and actin regulatory functions *in vivo*. However, during some processes, the two sub-families colocalize and appear to control actin assembly cooperatively (Bierne et al., 2005; Unsworth et al., 2004). The WAVEs function within an assembly also containing Sra1, Nap1, Abi and HSPC300 (Eden et al., 2002). The isolated Abi protein can also bind and activate N-WASP through its SH3 domain (Innocenti et al., 2005).

We found that a trimeric sub-assembly containing Abi, HSPC300 and WAVE1 has appreciable activity toward Arp2/3 complex (Fig. 6B). We asked whether this trimer, as a model for the activated WAVE complex pentamer, could produce a high potency heterodimeric VCA through binding active N-WASP (N-$WASP_{BC}$*). Individually, trimer and N-$WASP_{BC}$* have only weak activity, but a mixture of the two is highly active (Fig. 6B). This hyperactivation requires binding of trimer to N-$WASP_{BC}$*, since it is not observed for mixtures of trimer with N-WASP VCA or WAVE1 VCA with N-$WASP_{BC}$* (Fig. 6B). Hyperactivation also requires the presence of two VCAs in the complex, since it is not observed in a mixture of trimer with a truncated N-WASP lacking the VCA (Fig. S14). Thus, formation of WAVE1:N-WASP heterodimers can produce high-potency activation. This effect may allow cooperativity between N-WASP and WAVE.

DISCUSSION

Hierarchical Regulation of WASP/WAVE Proteins

We have shown here that dimerization of WASP protein VCA elements increases affinity for Arp2/3 complex by 100–200-fold due to bi-valent VCA interactions with two distinct sites on the complex (Fig. 7). Dimerization greatly increases WASP activity *in vitro* and can control actin assembly during bacterial infection. This effect provides a common mechanistic framework that can now explain the behaviors of a range of apparently disparate multivalent WASP family ligands. Three independent agents capable of interacting with multiple WASP proteins, EspFu, SH3 dimers and PIP_2-containing vesicles show similar activity profiles, which agree with three modeling predictions (Fig. 3 and Fig. 4). First, each raises the activity of N-WASP well above that of its isolated VCA, indicating that they engage mechanisms distinct

from allosteric relief of autoinhibition. Independence from allostery is also supported by data on SH3 proteins and PIP_2, where hyperactivation is observed with constitutively active N-WASP mutants. For EspFu and SH3 proteins, the ability to hyperactivate depends critically on the presence of multiple WASP-binding sites; mono-valent proteins do not hyperactivate. Similarly, hyperactivation by PIP_2 is only observed for high density vesicles, where VCAs are likely at sufficient density to behave as oligomers. Second, in titrations with multi-valent EspFu and SH3 proteins, we observed bell-shaped activation of the N-WASP-Arp2/3 pathway. This shape is most pronounced for EspFu, which has only a single binding site on WASP (the GBD) and interacts with much higher affinity. Finally, hyperactivation is eliminated by agents that disrupt WASP multimers—EspFu 2R by 1R, dimeric SH3 proteins by monomeric SH3 proteins, and dilution of PIP_2 within individual vesicles. Together, these data strongly support the notion that dimerization/oligomerization of WASP family proteins is a general and widely used mechanism of controlling WASP activity toward Arp2/3 complex.

These findings lead to a new, hierarchical model for regulation of WASP/WAVE proteins (Fig. 7). In this model, WASP activity is controlled by two mechanistically distinct processes. An inner layer of allostery controls accessibility of the VCA. In WASP, this occurs through autoinhibitory GBD-VCA interactions. In WAVE, this occurs through intersubunit interactions in the Sra1/Nap1/Abi/HSPC300/WAVE assembly (A.M.I. and M.K.R., unpublished; (Eden et al., 2002)). For both WASP and WAVE, exposure of the VCA (through presently unknown mechanisms for the latter) produces a monomeric species with micromolar affinity for Arp2/3 complex. This allosteric layer lies under a second layer of regulation, in which dimerization greatly increases affinity for Arp2/3 complex. Thus, when WASP protein concentrations are low, dimerization can potently enhance activity towards Arp2/3 complex. Dimerization can occur through assembly by multi-valent protein ligands and/or recruitment to high density at membranes. The system is genuinely hierarchical, since dimerization of completely autoinhibited WASP will not enable Arp2/3 stimulation. For example, the dimeric SH3-containing N-WASP ligand, Toca-1, cannot activate the strongly inhibited N-WASP:WIP complex, except when Cdc42 partially relieves autoinhibition (Ho et al., 2004). As detailed in the supplementary materials, the second layer of regulation provided by dimerization will increase the inherent complexity afforded by the WASP allosteric switch.

Higher Order Oligomerization as a Probabilistic Potentiator of Allosteric Activation

A large variety of data have shown that increasing the local density of components of Arp2/3 regulatory pathways can increase actin assembly *in vitro* and *in vivo*. Membrane recruitment and complex formation through repetitive interaction modules (e.g. SH3 domains and proline-rich motifs) produces Arp2/3-dependent assembly of actin filament networks in cells and in biochemical reconstitutions (Alto et al., 2007; Castellano et al., 2000; Itoh et al., 2005; Rivera et al., 2004; Tehrani et al., 2007; Tsujita et al., 2006; Yarar et al., 2007). These complexes likely contain multiple WASP proteins. For example, PCH proteins create actin coated membrane tubules by forming close-packed arrays on lipid surfaces which recruit N-WASP (Frost et al., 2008; Shimada et al., 2007). We suggest that dimerization can explain enhanced actin assembly in these different systems.

Dimerization increases the activity of N-WASP toward Arp2/3 complex even when the linker between VCAs is very long. In complex with EspFu 2R and PACSIN2, the VCAs of active N-WASP are separated by at least 8 nm and 16 nm (assuming random coil between the F-BAR and SH3 domains), respectively (Cantor and Schimmel, 1980). On PCH domain induced membrane tubules, N-WASP is recruited by SH3 domains, which have an average spacing of ~7 nM (Frost et al., 2008) (Itoh et al., 2005; Tsujita et al., 2006). Thus, within assemblies, VCA pairs should be capable of acting cooperatively in binding to Arp2/3 complex. Similar arguments hold for Arp2/3 activators at high density on membranes, such as N-WASP on

rocketing vesicles (Co et al., 2007) or ActA on the surface of Listeria (Footer et al., 2008). In a cluster containing n independently regulated WASP proteins, each with a probability P_m of being allosterically activated, the probability of at least two WASPs being active simultaneously, P_d, increases with n (Fig. 5B, relationship between P_d, P_m and n given by Eq. S25, see Supplementary Materials). Allosteric activators act on such a cluster by increasing P_m, changing activity (as measured by P_d) according to a vertical shift in Figure 5B. However, factors that simply increase the size of an assembly, n, will also serve as activators, causing a rightward shift in Fig. 5B. This effect is conceptually analogous to the enhanced activity observed upon increasing the number of WASP-binding repeats in EspFu at a fixed total repeat concentration (Fig. 5A) (See Supplementary Materials). In the case of assemblies, oligomerizing and allosteric inputs should show strong synergy.

Finally, we note that this implies that larger complexes will have more activity toward Arp2/3 complex, and thus more locally produced actin filaments. Taunton and colleagues have shown that the V region of N-WASP can bind filament barbed ends, and that this interaction is necessary for attachment of actin networks to moving membranes (Co et al., 2007). They suggested that this effect could enable the actin network to capture, and thus locally concentrate, diffusing WASP proteins, resulting in localized signal amplification. The dimerization effect that we have described here could act synergistically with this mechanism by enhancing Arp2/3 recruitment by the concentrated WASP proteins. At a molecular level, the two mechanisms suggest that membranebound WASP proteins associated with a dendritic array could have segregated functions, some binding barbed ends, others activating Arp2/3. Such functional segregation could also occur among VCAs in dimeric/oligomeric assemblies. Together, these activities would give localized high-affinity Arp2/3 activation while maintaining attachment of the network to membranes.

EXPERIMENTAL PROCEDURES

Generation of Materials

Detailed expression and purification procedures for all materials are provided in Table S1 and the Supplementary Materials. Generally, proteins were expressed in *E. coli* strain BL21(DE3) $T1^R$, and purified using a combination of affinity and conventional chromatographies.

Actin Assembly Assays

All actin assembly assays except those used for kinetic modeling (see Supplementary Materials) contained 4 μM actin (5% pyrene labeled) and 10 nM Arp2/3 complex in either KMEI or 150KMEI buffer as indicated in the figure legends, and were performed as described (Leung et al., 2006). KMEI contains 50 mM KCl (150 mM in 150KMEI), 1 mM $MgCl_2$, 1 mM EGTA, and 10 mM Imidazole pH 7.0. Observation of hyperactivation required the use of freshly purified Arp2/3 complex. Relative activities of actin polymerization assays were quantified as t_{50}(VCA)/t_{50}, the time at which one half of the actin has polymerized (t_{50}) in a VCA reference sample, divided by t_{50} for the sample in question. Quantification using filament barbed ends concentration produced qualitatively identical results. Data shown in figure 1, figure 4, figure 5 and figure 6 are representative of at least two repeats of experiments.

EspFu Dependent Pedestal Assays

For experiments involving actin assembly by EspFu, mouse fibroblast-like cells were transfected with HA-Tir-EspFu fusions, treated with intimin-expressing E. coli for 3.5 hours, and then fixed, permeabilized and stained for Tir and F-actin as described (Cheng et al., 2008).

Arp2/3 Affinity Measurements

VCA and NtA affinities for Arp2/3 complex were determined using a competition binding assay based on the fluorescence anisotropy of rhodamine-labeled N-WASP VCA (rVCA) or rhodamine-labeled cortactin NtA (rNta) (Marchand et al., 2001). Anisotropy data were fit to a full solution of equilibrium competition binding (See Supplementary Materials).

Arp2/3 Pulldowns

HEK293 cells were transfected using Lipofectamine 2000 with plasmids encoding FKBP-WASP VCA-His_6 (2.0 μg, pCMV) or His_6-FKBP (2.0 μg, pCMV) and mTOR-WASP VCA-FLAG with a C-terminal FLAG tag (2.0 μg, pCMV). Cells were treated with 5 μM rapamycin or DMSO carrier, harvested by scraping and lysed in 0.05% Triton-X in 50 mM Tris-Cl (pH 7.5) with 50 mM NaCl. Each sample was a pool of six identical wells. Complexes retained on Ni-NTA agarose (Qiagen) were detected by western blotting against Arp3 (Arp3(A-1), Santa Cruz), FLAG-tag (Anti-FLAG M2, SIGMA) or His_6-tag (His-Probe (H-3), Santa Cruz), visualized by goat anti-mouse IgG (H+L)-HRP conjugate (Bio-Rad) secondary antibodies. Data shown are representative of two independent experiments.

Modeling of WASP/Dimerizer/Arp2/3 Equilibria

We modeled the concentration of active Arp2/3 complex according to the binding equilibria for WASP, dimerizer, monomeric dimerizer and Arp2/3 described by equations S17–S24, which were solved iteratively. An affinity of 1 μM was used for dimerizer binding to WASP and monomeric WASP binding to Arp2/3. Dimeric WASP bound Arp2/3 with an affinity of 10 nM. Equations and additional details are provided in Supplementary materials.

Analytical Ultracentrifugation

Analytical velocity sedimentation experiments were performed in an XL-I ultracentrifuge (Beckman-Coulter) using sapphire-windowed, dual-sectored cells in an An60-Ti rotor. Sedimentation at 20°C, 42,000 rpm in KMEI was recorded using both absorbance (280 nm) and interferometric optics. SEDFIT (Schuck et al., 2002) was used to derive continuous $c(s)$ distributions from the sedimentation velocity data. Protein and buffer parameters were estimated using SEDNTERP (Laue et al., 1992). Component masses were determined using Svedberg's equation from values of s and f/f_0 (see Supplemental Materials).

Multi-Angle Static Light Scattering

Arp2/3 complex and GST-WASP VCA were mixed in a 1:3 ratio (i.e. 1:1.5 Arp2/3:VCA dimer). The mixture was injected onto a Superdex200 gel filtration column connected in line to a DAWN EOS light scattering instrument, a 690 nm laser and OPTILAB DSP interferometric refractometer. Data were analyzed with ASTRA software (Wyatt Technology Corporation).

Lipid Cosedimentation

Cosedimentation of N-$WASP_B$ with sucrose loaded PIP_2 vesicles was performed in KMEI plus 10 mM sucrose. Samples were centrifuged at 175,000 *g* for one hour and quantified by the fraction of stained band intensity in the pellet fraction (see Supplementary Materials).

Supplementary Material

Refer to Web version on PubMed Central for supplementary material.

ACKNOWLEDGEMENTS

We thank Dr. Luke Rice and Pilong Li for advice regarding modeling, Tim Craig and Drs. Joe Albanesi and Elliott Ross for assistance with lipid experiments, Dr. Hongtao Yu for assistance with cell culture, Dr. Tom Wandless for providing rapamycin, Drs. Daisy Leung and Xiaolan Yao for providing mTOR and FKBP expression constructs, Chinatsu Otomo for cloning assistance and Dr. Tom Pollard for critical review of the manuscript. This work was supported by the Howard Hughes Medical Institute and grants from the NIH (NIH-R01-GM56322 to M.K.R.; NIH-R01-AI46454 to J.L.), and Welch Foundation (I–1544 to M.K.R.). S. B. P. and H.-C. C. were supported by fellowships from the NIH (1F32-GM06917902), and the Chilton Foundation, respectively.

REFERENCES

Alto NM, Weflen AW, Rardin MJ, Yarar D, Lazar CS, Tonikian R, Koller A, Taylor SS, Boone C, Sidhu SS, et al. The type III effector EspF coordinates membrane trafficking by the spatiotemporal activation of two eukaryotic signaling pathways. J Cell Biol 2007;178:1265–1278. [PubMed: 17893247]

Banaszynski LA, Liu CW, Wandless TJ. Characterization of the FKBP.rapamycin.FRB ternary complex. J Am Chem Soc 2005;127:4715–4721. [PubMed: 15796538]

Bierne H, Miki H, Innocenti M, Scita G, Gertler FB, Takenawa T, Cossart P. WASP-related proteins, Abi1 and Ena/VASP are required for Listeria invasion induced by the Met receptor. J Cell Sci 2005;118:1537–1547. [PubMed: 15769844]

Campellone KG, Robbins D, Leong JM. EspFU is a translocated EHEC effector that interacts with Tir and N-WASP and promotes Nck-independent actin assembly. Dev Cell 2004;7:217–228. [PubMed: 15296718]

Campellone KG, Webb NJ, Znameroski EA, Welch MD. WHAMM is an Arp2/3 complex activator that binds microtubules and functions in ER to Golgi transport. Cell 2008;134:148–161. [PubMed: 18614018]

Cantor, CR.; Schimmel, PR. Biophysical Chemistry, Part III: The Behavior of Biological Macromolecules. New York: W. H. Freeman and Company; 1980.

Castellano F, Montcourrier P, Chavrier P. Membrane recruitment of Rac1 triggers phagocytosis. J Cell Sci 2000;113(Pt 17):2955–2961. [PubMed: 10934035]

Castellano F, Montcourrier P, Guillemot JC, Gouin E, Machesky L, Cossart P, Chavrier P. Inducible recruitment of Cdc42 or WASP to a cell-surface receptor triggers actin polymerization and filopodium formation. Curr Biol 1999;9:351–360. [PubMed: 10209117]

Cheng H-C, Skehan BM, Campellone KG, Leong JM, Rosen MK. Structural Mechanism of WASP Activation by the Enterohaemorrhagic E. Coli Effector EspFu. Nature 2008;4541009-1001-1013

Chhabra ES, Higgs HN. The many faces of actin: matching assembly factors with cellular structures. Nat Cell Biol 2007;9:1110–1121. [PubMed: 17909522]

Co C, Wong DT, Gierke S, Chang V, Taunton J. Mechanism of actin network attachment to moving membranes: barbed end capture by N-WASP WH2 domains. Cell 2007;128:901–913. [PubMed: 17350575]

Devriendt K, Kim AS, Mathijs G, Frints SG, Schwartz M, Van Den Oord JJ, Verhoef GE, Boogaerts MA, Fryns JP, You D, et al. Constitutively activating mutation in WASP causes X-linked severe congenital neutropenia. Nat Genet 2001;27:313–317. [PubMed: 11242115]

Eden S, Rohatgi R, Podtelejnikov AV, Mann M, Kirschner MW. Mechanism of regulation of WAVE1-induced actin nucleation by Rac1 and Nck. Nature 2002;418:790–793. [PubMed: 12181570]

Footer MJ, Lyo JK, Theriot JA. Close packing of listeria monocytogenes acta, a natively unfolded protein, enhances F-actin assembly without dimerization. J Biol Chem. 2008

Frost A, Perera R, Roux A, Spasov K, Destaing O, Egelman EH, De Camilli P, Unger VM. Structural basis of membrane invagination by F-BAR domains. Cell 2008;132:807–817. [PubMed: 18329367]

Fukuoka M, Suetsugu S, Miki H, Fukami K, Endo T, Takenawa T. A novel neural Wiskott-Aldrich syndrome protein (N-WASP) binding protein, WISH, induces Arp2/3 complex activation independent of Cdc42. J Cell Biol 2001;152:471–482. [PubMed: 11157975]

Garmendia J, Carlier MF, Egile C, Didry D, Frankel G. Characterization of TccP-mediated N-WASP activation during enterohaemorrhagic Escherichia coli infection. Cell Microbiol 2006;8:1444–1455. [PubMed: 16922863]

Garmendia J, Phillips AD, Carlier MF, Chong Y, Schuller S, Marches O, Dahan S, Oswald E, Shaw RK, Knutton S, Frankel G. TccP is an enterohaemorrhagic Escherichia coli O157:H7 type III effector protein that couples Tir to the actin-cytoskeleton. Cell Microbiol 2004;6:1167–1183. [PubMed: 15527496]

Garmendia J, Ren Z, Tennant S, Midolli Viera MA, Chong Y, Whale A, Azzopardi K, Dahan S, Sircili MP, Franzolin MR, et al. Distribution of tccP in clinical enterohemorrhagic and enteropathogenic Escherichia coli isolates. J Clin Microbiol 2005;43:5715–5720. [PubMed: 16272509]

Goley ED, Welch MD. The ARP2/3 complex: an actin nucleator comes of age. Nat Rev Mol Cell Biol 2006;7:713–726. [PubMed: 16990851]

Higgs HN, Pollard TD. Activation by Cdc42 and PIP(2) of Wiskott-Aldrich syndrome protein (WASp) stimulates actin nucleation by Arp2/3 complex. J Cell Biol 2000;150:1311–1320. [PubMed: 10995437]

Ho HY, Rohatgi R, Lebensohn AM, Le M, Li J, Gygi SP, Kirschner MW. Toca-1 mediates Cdc42-dependent actin nucleation by activating the N-WASP-WIP complex. Cell 2004;118:203–216. [PubMed: 15260990]

Innocenti M, Gerboth S, Rottner K, Lai FP, Hertzog M, Stradal TE, Frittoli E, Didry D, Polo S, Disanza A, et al. Abi1 regulates the activity of N-WASP and WAVE in distinct actin-based processes. Nat Cell Biol 2005;7:969–976. [PubMed: 16155590]

Itoh T, Erdmann KS, Roux A, Habermann B, Werner H, De Camilli P. Dynamin and the actin cytoskeleton cooperatively regulate plasma membrane invagination by BAR and F-BAR proteins. Dev Cell 2005;9:791–804. [PubMed: 16326391]

Kim AS, Kakalis LT, Abdul-Manan N, Liu GA, Rosen MK. Autoinhibition and activation mechanisms of the Wiskott-Aldrich syndrome protein. Nature 2000;404:151–158. [PubMed: 10724160]

Laue, TM.; Shah, BD.; Ridgeway, RM.; Pelletier, SL. Computer-aided interpretation of analytical sedimentation data for proteins. In: Harding, SE.; Rowe, AJ.; Horton, JC., editors. Analytical Ultracentrifugation in Biochemistry and Polymer Science. Cambridge, UK: The Royal Society of Chemistry; 1992.

Leung DW, Morgan DM, Rosen MK. Biochemical properties and inhibitors of (N-)WASP. Methods Enzymol 2006;406:281–296. [PubMed: 16472665]

Leung DW, Rosen MK. The Nucleotide Switch in Cdc42 Modulates Coupling Between the GTPase-Binding and Allosteric Equilibria of WASP. Proc Natl Acad Sci U S A 2005;102:5685–5690. [PubMed: 15821030]

Linardopoulou EV, Parghi SS, Friedman C, Osborn GE, Parkhurst SM, Trask BJ. Human Subtelomeric WASH Genes Encode a New Subclass of the WASP Family. PLoS Genet 2007;3:e237. [PubMed: 18159949]

Marchand JB, Kaiser DA, Pollard TD, Higgs HN. Interaction of WASP/Scar proteins with actin and vertebrate Arp2/3 complex. Nat Cell Biol 2001;3:76–82. [PubMed: 11146629]

Miki H, Sasaki T, Takai Y, Takenawa T. Induction of filopodium formation by a WASP-related actin-depolymerizing protein N-WASP. Nature 1998;391:93–96. [PubMed: 9422512]

Miller WG, Brant DA, Flory PJ. Random Coil Configurations of Polypeptide Copolymers. J Mol Biol 1967;23:67–80.

Munter S, Way M, Frischknecht F. Signaling during pathogen infection. Sci STKE 2006;2006:re5. [PubMed: 16705131]

Ochs HD, Thrasher AJ. The Wiskott-Aldrich syndrome. J Allergy Clin Immunol 2006;117:725–738. [PubMed: 16630926]quiz 739

Papayannopoulos V, Co C, Prehoda KE, Snapper S, Taunton J, Lim WA. A polybasic motif allows N-WASP to act as a sensor of PIP(2) density. Mol Cell 2005;17:181–191. [PubMed: 15664188]

Peterson JR, Bickford LC, Morgan D, Kim AS, Ouerfelli O, Kirschner MW, Rosen MK. Chemical inhibition of N-WASP by stabilization of a native autoinhibited conformation. Nat Struct Mol Biol 2004;11:747–755. [PubMed: 15235593]

Pollard TD. Regulation of actin filament assembly by Arp2/3 complex and formins. Annu Rev Biophys Biomol Struct 2007;36:451–477. [PubMed: 17477841]

Pollard TD, Borisy GG. Cellular motility driven by assembly and disassembly of actin filaments: Integration of signals to the Arp2/3 complex. Cell 2003;112:453–465. [PubMed: 12600310]

Prehoda KE, Scott JA, Mullins RD, Lim WA. Integration of multiple signals through cooperative regulation of the N- WASP-Arp2/3 complex. Science 2000;290:801–806. [PubMed: 11052943]

Rivera GM, Briceno CA, Takeshima F, Snapper SB, Mayer BJ. Inducible clustering of membrane-targeted SH3 domains of the adaptor protein Nck triggers localized actin polymerization. Curr Biol 2004;14:11–22. [PubMed: 14711409]

Rohatgi R, Ho HY, Kirschner MW. Mechanism of N-WASP activation by CDC42 and phosphatidylinositol 4, 5- bisphosphate. J Cell Biol 2000;150:1299–1310. [PubMed: 10995436]

Rohatgi R, Ma L, Miki H, Lopez M, Kirchhausen T, Takenawa T, Kirschner MW. The interaction between N-WASP and the Arp2/3 complex links Cdc42-dependent signals to actin assembly. Cell 1999;97:221–231. [PubMed: 10219243]

Rohatgi R, Nollau P, Ho HY, Kirschner MW, Mayer BJ. Nck and phosphatidylinositol 4,5-bisphosphate synergistically activate actin polymerization through the N-WASP-Arp2/3 pathway. J Biol Chem 2001;276:26448–26452. [PubMed: 11340081]

Sallee NA, Rivera GM, Dueber JE, Vasilescu D, Mullins RD, Mayer BJ, Lim WA. The pathogen protein EspF(U) hijacks actin polymerization using mimicry and multivalency. Nature. 2008

Schuck P, Perugini MA, Gonzales NR, Howlett GJ, Schubert D. Size-distribution analysis of proteins by analytical ultracentrifugation: strategies and application to model systems. Biophys J 2002;82:1096–1111. [PubMed: 11806949]

Shimada A, Niwa H, Tsujita K, Suetsugu S, Nitta K, Hanawa-Suetsugu K, Akasaka R, Nishino Y, Toyama M, Chen L, et al. Curved EFC/F-BAR-domain dimers are joined end to end into a filament for membrane invagination in endocytosis. Cell 2007;129:761–772. [PubMed: 17512409]

Stradal TE, Scita G. Protein complexes regulating Arp2/3-mediated actin assembly. Curr Opin Cell Biol 2006;18:4–10. [PubMed: 16343889]

Suetsugu S, Miki H, Takenawa T. Identification of another actin-related protein (arp) 2/3 complex binding site in neural wiskott-aldrich syndrome protein (n-wasp) that complements actin polymerization induced by the arp2/3 complex activating (vca) domain of n-wasp. J Biol Chem 2001;276:33175–33180. [PubMed: 11432863]

Takenawa T, Suetsugu S. The WASP-WAVE protein network: connecting the membrane to the cytoskeleton. Nat Rev Mol Cell Biol 2007;8:37–48. [PubMed: 17183359]

Tehrani S, Tomasevic N, Weed S, Sakowicz R, Cooper JA. Src phosphorylation of cortactin enhances actin assembly. Proc Natl Acad Sci U S A 2007;104:11933–11938. [PubMed: 17606906]

Torres E, Rosen MK. Contingent phosphorylation/dephosphorylation provides a mechanism of molecular memory in WASP. Mol Cell 2003;11:1215–1227. [PubMed: 12769846]

Tsujita K, Suetsugu S, Sasaki N, Furutani M, Oikawa T, Takenawa T. Coordination between the actin cytoskeleton and membrane deformation by a novel membrane tubulation domain of PCH proteins is involved in endocytosis. J Cell Biol 2006;172:269–279. [PubMed: 16418535]

Unsworth KE, Way M, McNiven M, Machesky L, Holden DW. Analysis of the mechanisms of Salmonella-induced actin assembly during invasion of host cells and intracellular replication. Cell Microbiol 2004;6:1041–1055. [PubMed: 15469433]

Weaver AM, Heuser JE, Karginov AV, Lee WL, Parsons JT, Cooper JA. Interaction of cortactin and N-WASp with Arp2/3 complex. Curr Biol 2002;12:1270–1278. [PubMed: 12176354]

Yamazaki D, Kurisu S, Takenawa T. Regulation of cancer cell motility through actin reorganization. Cancer Sci 2005;96:379–386. [PubMed: 16053508]

Yarar D, Waterman-Storer CM, Schmid SL. SNX9 couples actin assembly to phosphoinositide signals and is required for membrane remodeling during endocytosis. Dev Cell 2007;13:43–56. [PubMed: 17609109]

Zalevsky J, Lempert L, Kranitz H, Mullins RD. Different WASP family proteins stimulate different Arp2/3 complex- dependent actin-nucleating activities. Curr Biol 2001;11:1903–1913. [PubMed: 11747816]

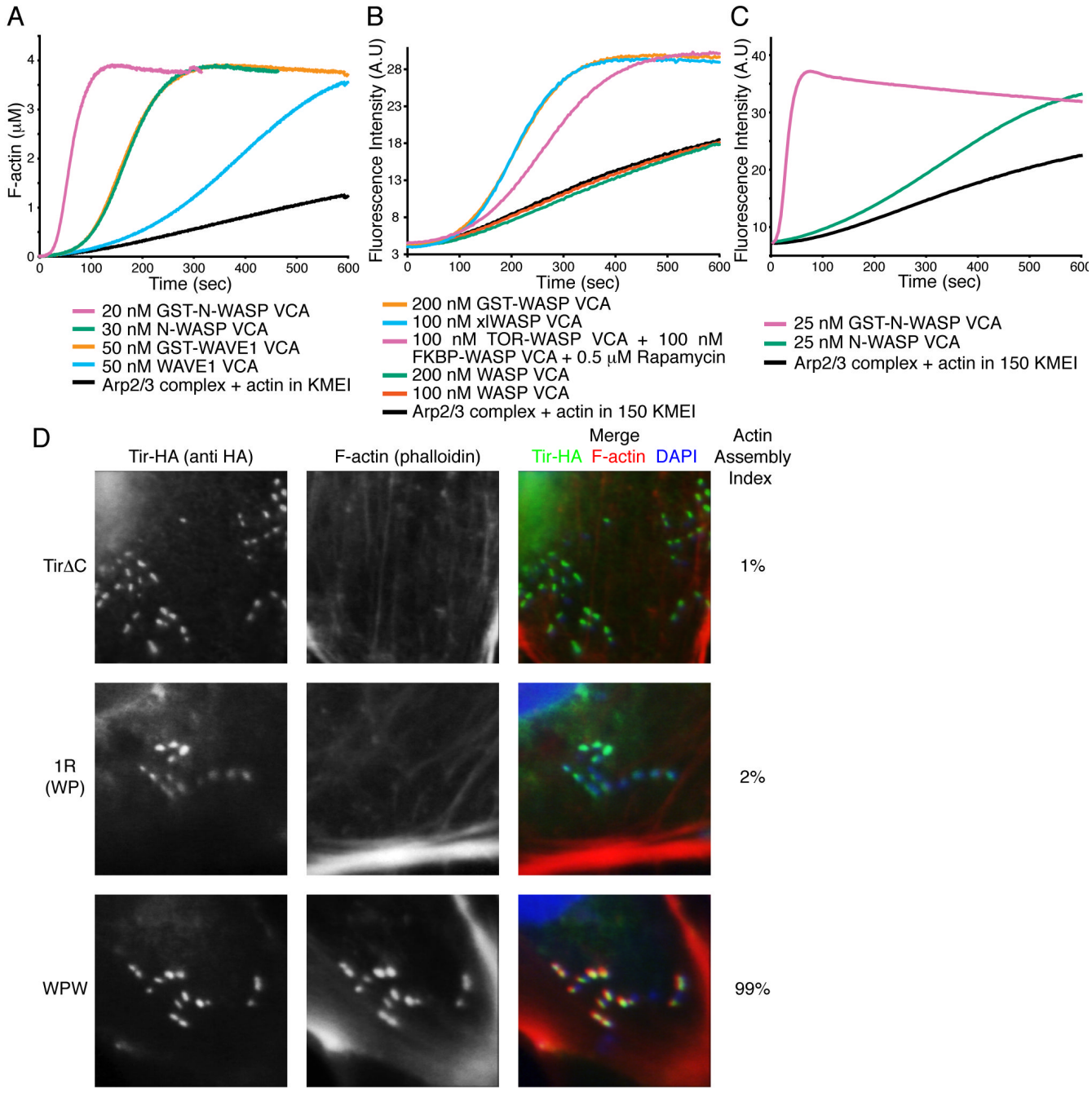

Figure 1. Dimerization Increases VCA Activity *In Vitro* and in Cells

(A – C) Pyrene fluorescence measured during assembly of actin by Arp2/3 complex (black) plus the indicated components. Without rapamycin, 100 nM mTOR-WASP VCA + 100 nM FKBP-WASP VCA has activity comparable to 200 nM WASP VCA (not shown). (D) Clustered EspFu leads to actin rich pedestal formation, but requires the ability to recruit multiple WASP molecules. Cells expressing HA-tagged TirΔC, TirΔC-1R (WP) or TirΔC-WPW were treated with intimin-expressing *E. coli*, and stained with anti-HA antibody (green in merged image) and Alexa568-phalloidin (red in merged image). Colocalization is yellow in merged image. The fraction of transfected cells harboring at least five F-actin foci was quantified (Actin Assembly Index). Bacteria were visualized by DAPI staining (blue in merged

image). Data represent mean from three independent samples of 30 cells each, standard deviation for all samples is 2%.

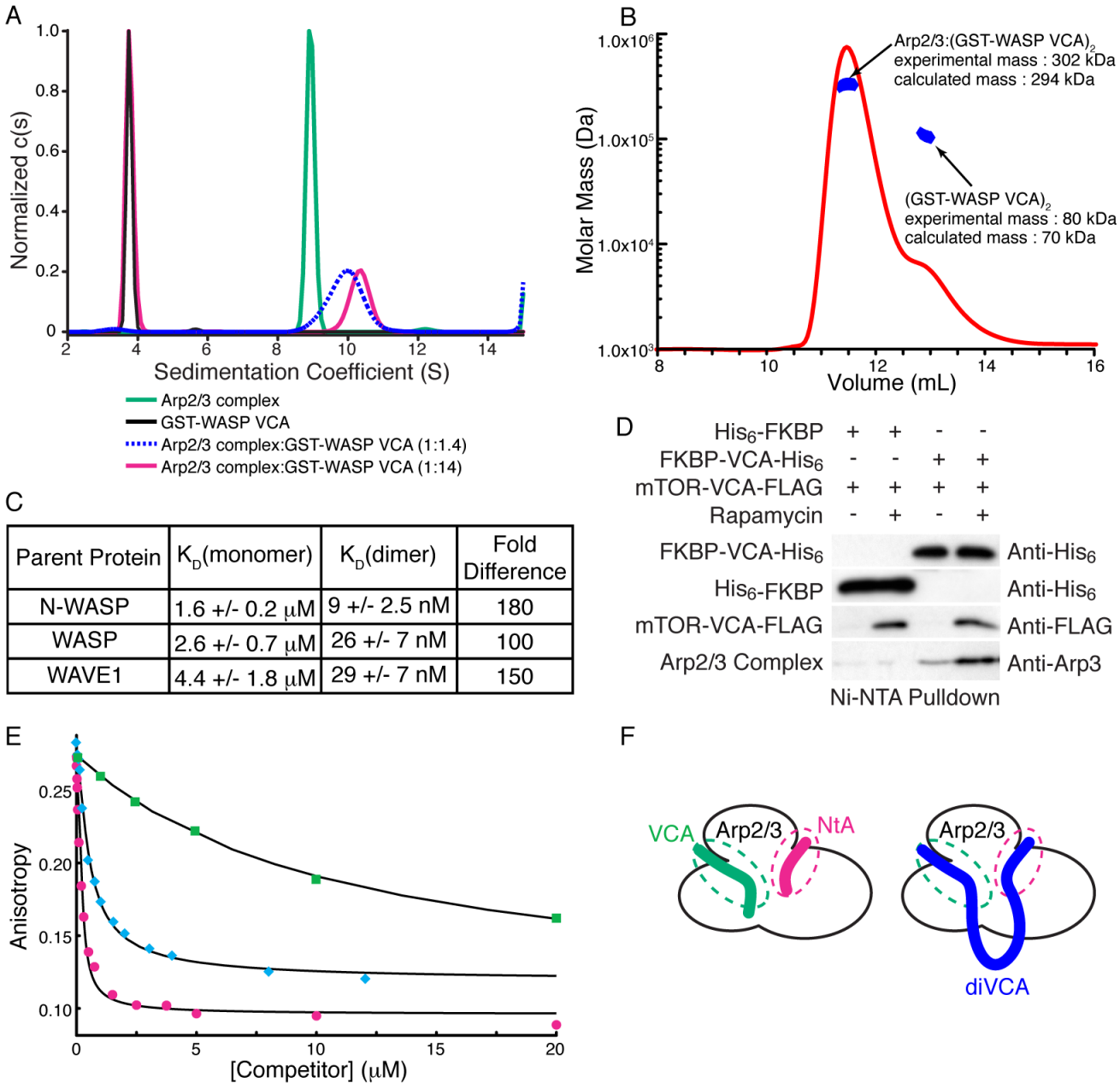

Parent Protein	K_D(monomer)	K_D(dimer)	Fold Difference
N-WASP	1.6 +/- 0.2 μM	9 +/- 2.5 nM	180
WASP	2.6 +/- 0.7 μM	26 +/- 7 nM	100
WAVE1	4.4 +/- 1.8 μM	29 +/- 7 nM	150

Figure 2. VCA Dimers Bind Arp2/3 with 1:1 Stoichiometry and High Affinity

(A) Normalized *c(s)* distributions from sedimentation velocity ultracentrifugation analyses of GST-WASP VCA (black), Arp2/3 complex (green), and Arp2/3 complex + GST-WASP VCA (0.5 μM + 6.8 μM, magenta; 1.8 μM + 2.6 μM, dashed blue). The black, green, and red distributions were normalized to a maximum *c*(*s*) value of 1.0; the blue distribution was normalized to give maximum *c*(*s*) value equal to that of the 10.3-S peak of the red distribution. (B) Molar mass distribution of multi-angle light scattering data collected on a 1:3 mixture of Arp2/3 complex and GST-WASP VCA, where excess GST-WASP VCA is resolved using Superdex200. Mass distribution within selected peaks is in blue, chromatogram is shown as red curve (refractive index change). (C) Dissociation constants (K_D) for the interaction of Arp2/3 complex with VCA monomers and GST-VCA dimers from N-WASP, WASP and

WAVE1. Errors shown are 1σ confidence intervals from fitting. (D) Dimerized VCA increases Arp2/3 complex binding in cells. HEK 293 cells transfected with the indicated constructs were treated with rapamycin or DMSO for 30 minutes and lysed. Complexes were precipitated with NiNTA affinity resin and analyzed by western blotting for the indicated proteins. (E) Competition displacement of cortactin from Arp2/3 complex. 10 nM rNtA was displaced from 200 nM Arp2/3 using the indicated concentrations of NtA (magenta circles), xlWASP VCA (cyan diamonds) or WASP VCA (green squares). Black curves are best fit solutions to the competition binding equilibrium equations (see Supplemental Materials). (F) Cartoon model of $(VCA)_2$ binding to two distinct sites on Arp2/3 complex. The cartoon does not show the exact location of the sites on Arp2/3, but merely the presence of two binding sites, both of which are engaged by di-VCA materials.

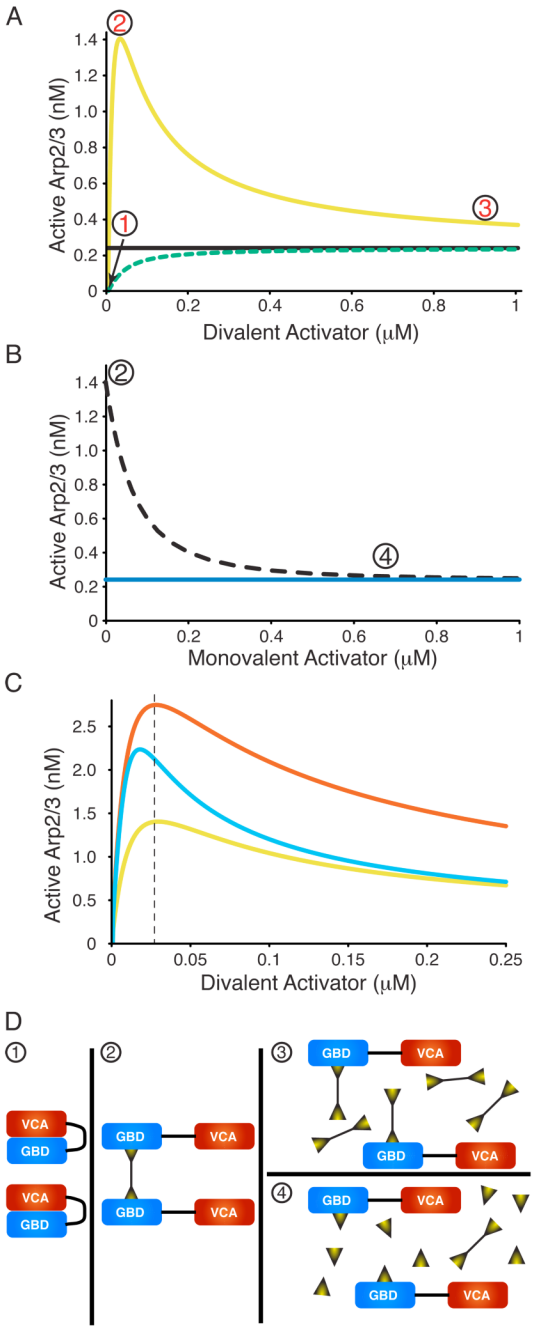

Figure 3. Modeling Predicts Unusual Behavior in Dimerizer Titrations

The concentration of active Arp2/3 complex was modeled as a function of dimerizing WASP ligands with different properties. Here, ligand binding is concomitant with allosteric relief of autoinhibition. See Figure S9 for ligands binding to constitutively active WASP ligands. (A) Simulated titrations of monomeric WASP ligand (dashed green, e.g. EspFu 1R) or dimeric WASP ligand (yellow, e.g. EspFu 2R) into WASP plus Arp2/3 complex. Black line indicates activity of VCA. (B) Simulated titration of monomeric WASP ligand (dotted black) into WASP hyperactivated by dimeric WASP ligand (maximum activity in A). Blue line indicates activity of VCA. (C) Simulated titrations of different dimerizing ligands into WASP plus Arp2/3 complex. Titration from (A) is yellow (note change of X- and Y-scales). Sky blue curve models

a dimerizer with 3-fold tighter affinity for WASP than in (A), red curve models a dimerizer: $(WASP)_2$ complex with three-fold tighter affinity for Arp2/3 than in (A). Modeling based on 25 nM WASP, 10 nM Arp2/3 complex throughout, and the following affinities in (A) and (B) —ligand:WASP, 30 nM; active monomeric WASP:Arp2/3, 1 μM; active dimeric WASP:Arp2/3, 10 nM. (D) Cartoons illustrating the relevant species during the activating dimerizer titrations. Circled numbers correspond to the states shown in (A) and (B).

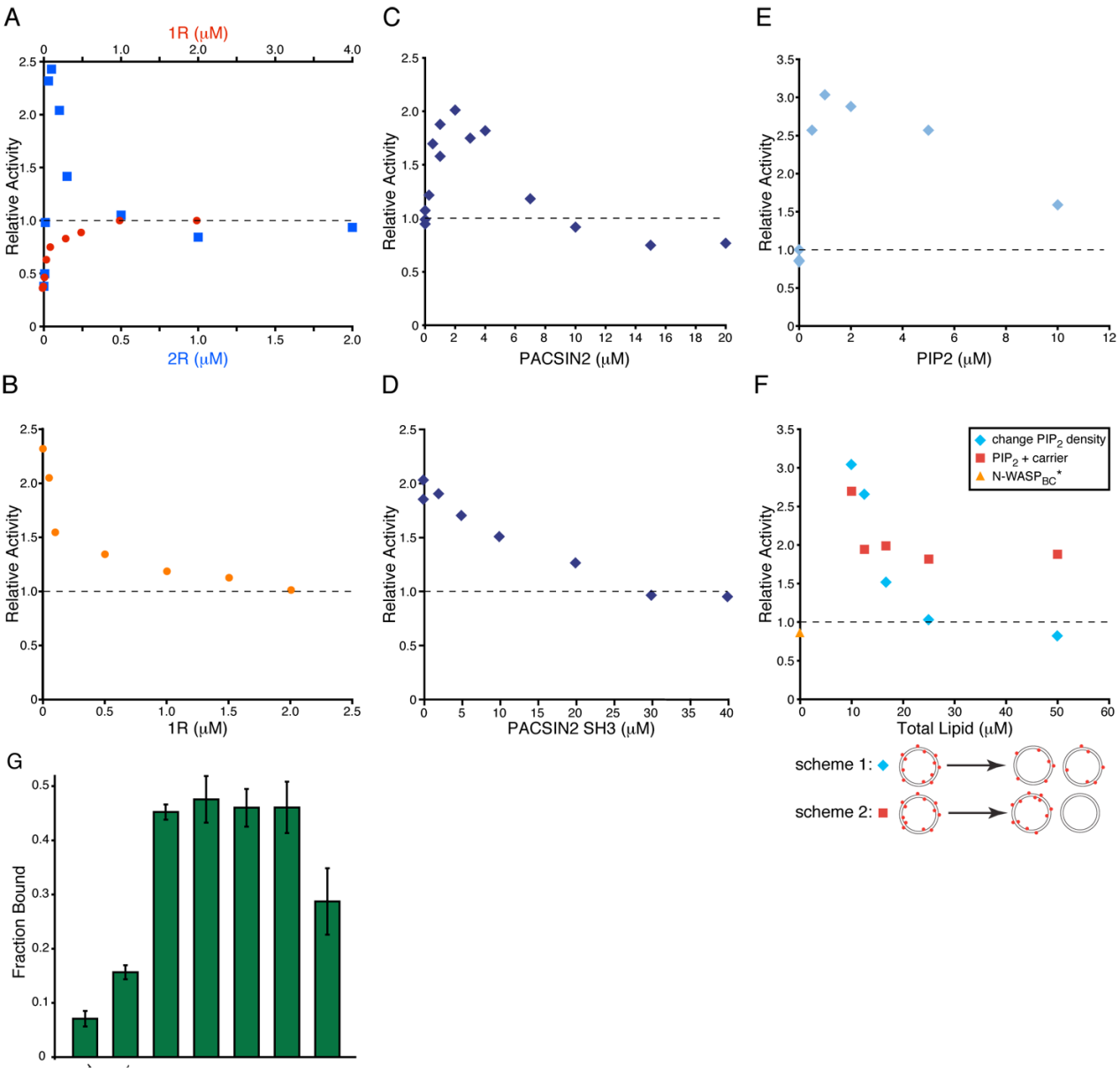

Figure 4. EspFu, SH3 Dimers and PIP2 Stimulate N-WASP Similarly

(A)–(F) Assembly of actin by Arp2/3 complex plus the indicated components, performed in KMEI. (A) Relative activity of 25 nM N-WASP$_C$ plus increasing concentrations of 1R (red circles) or 2R (blue squares), referenced to the activity of 25 nM N-WASP VCA (relative activity of 1, dashed line). (B) Relative activity of 25 nM N-WASP$_C$ + 50 nM 2R and increasing concentrations of 1R (orange circles). Relative activity defined as in (A). (C) Relative activity of 4 nM N-WASP$_C$* in the presence of increasing concentrations of PACSIN2, referenced to the activity of 4 nM N-WASP$_C$* (relative activity of 1, dashed line). (D) Relative activity of 4 nM N-WASP$_C$* + 3 μM PACSIN2 and increasing concentrations of PACSIN2-SH3. Dashed line as in (C). (E) Relative activity of 25 nM N-WASP$_{BC}$* in the presence of increasing concentrations of PIP$_2$ presented at high density (20 %) on vesicles, referenced to the activity of 25 nM N-WASP VCA (relative activity of 1, dashed line). (F) Relative activity of 25 nM N-WASP$_{BC}$* in the presence of 2 μM PIP$_2$ at varying total lipid concentration. In scheme 1, lipids are mixed such that PIP$_2$ density is uniform on all vesicles (blue diamonds), and in

scheme 2, high PIP_2 density vesicles are combined with carrier lipid vesicles to the same lipid concentrations as in scheme 1 (red squares) but PIP_2 and carrier lipids do not mix. Orange triangle shows 25 nM N-$WASP_{BC}$* alone. Dashed line as in (E). (G) Fraction of N-$WASP_B$ bound in lipid co-sedimentation assays. 200 nM N-$WASP_B$ was mixed with 5 μM PIP_2 vesicle and centrifuged. Total lipid for carrier experiment matches the 20% PIP_2 sample. Error bars are 1σ error estimated from at least three repeats.

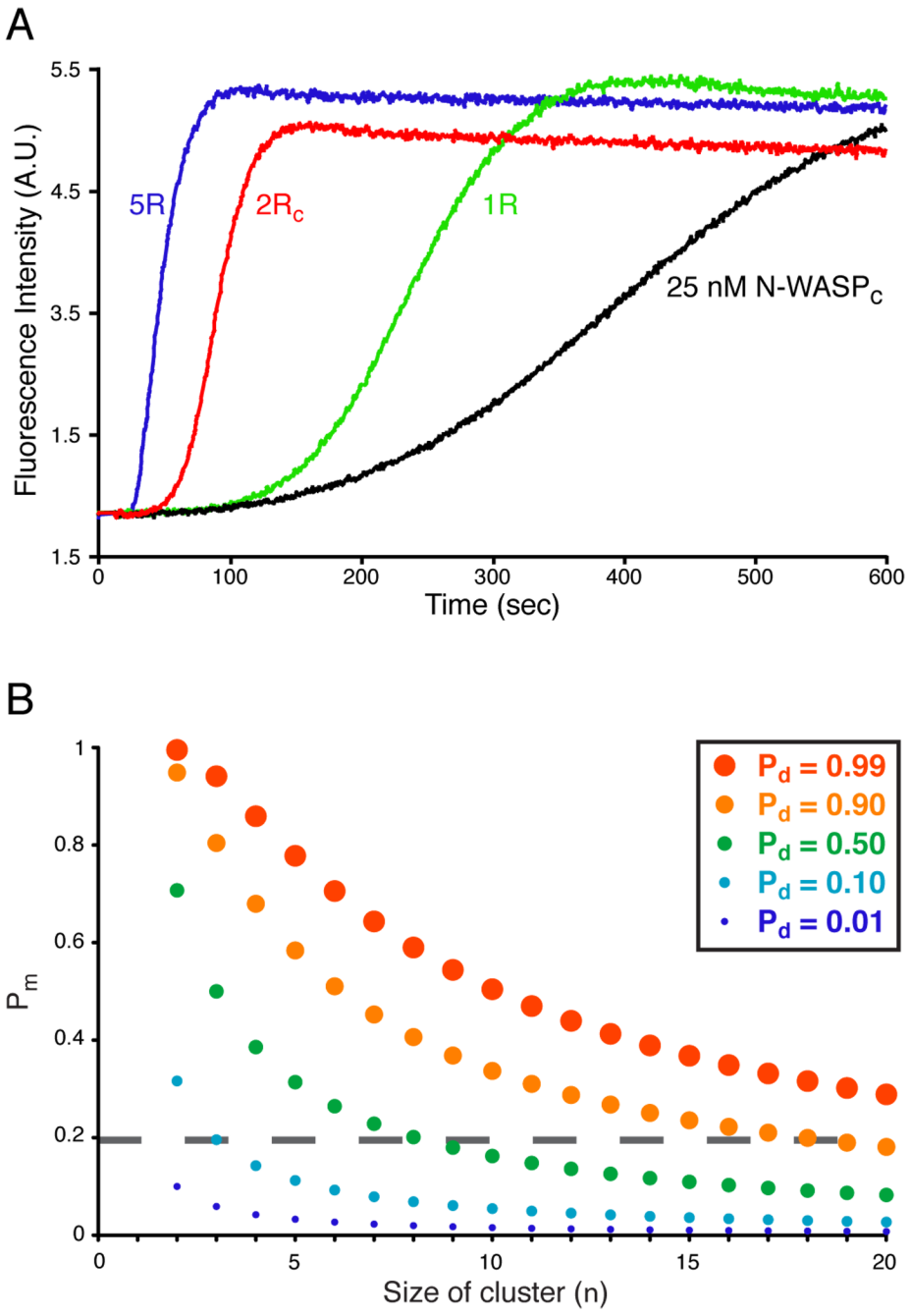

Figure 5. Increasing WASP Complex Size Increases Activity Probabilistically

(A) Pyrene-actin fluorescence measured during Arp2/3-mediated actin assembly in the presence of 25 nM N-WASP$_C$ alone (black) or plus 1 μM EspFu 1R (green), 500 nM 2R$_C$ (red) or 200 nM 5R (blue). Assay performed in KMEI. (B) Plot of the probabilities of obtaining a dimeric/oligomeric WASP species (P_d) as a function the probability of having a monomeric active WASP (P_m, Y-axis), and the size of the cluster formed by WASP dimerizers (n, X-axis).

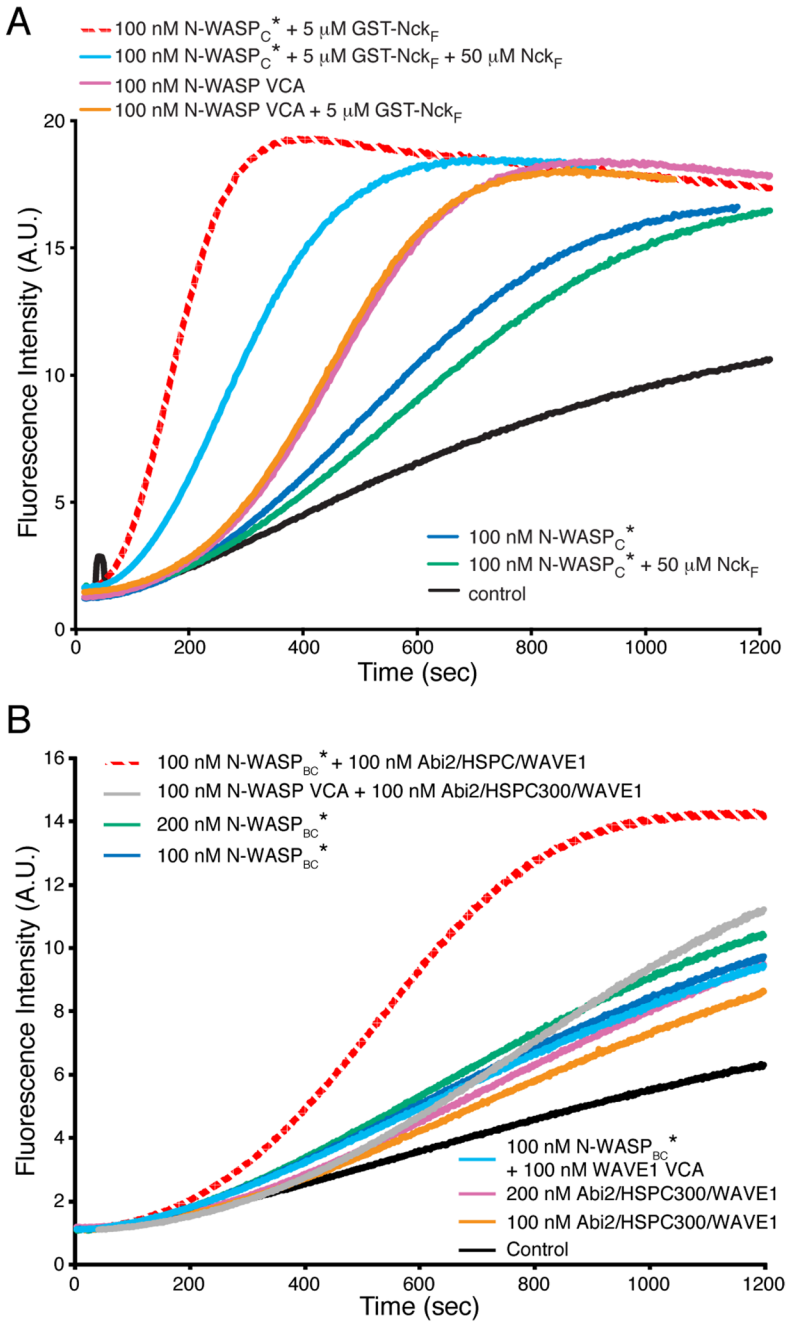

Figure 6. Hyperactivation by SH3-Mediated Homo- or Hetero-Dimerization

Pyrene-actin fluorescence measured during Arp2/3-mediated actin assembly in the presence of the indicated components. Control is actin + Arp2/3 complex. Assays performed in 150KMEI (A) or 150KMEI + 15%glycerol (B).

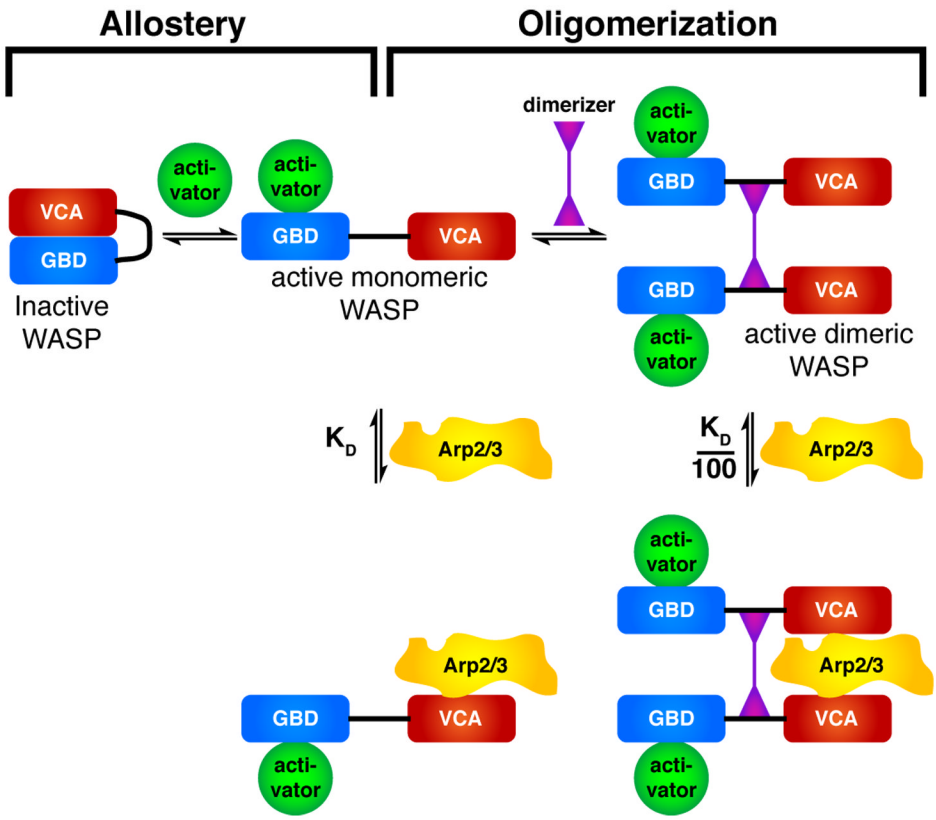

Figure 7. A Hierarchical model for WASP/WAVE regulation

An inner layer of allostery controls accessibility of the VCA element. An outer layer of dimerization, or more generally oligomerization, controls affinity of the active VCA for Arp2/3 complex.